Research Article

Which Biopolymers Are Better for the Fabrication of Multilayer Capsules? A Comparative Study Using Vaterite CaCO$_3$ as Templates

Jack Campbell, Jordan Abnett, Georgia Kastania, Dmitry Volodkin,* and Anna S. Vikulina*

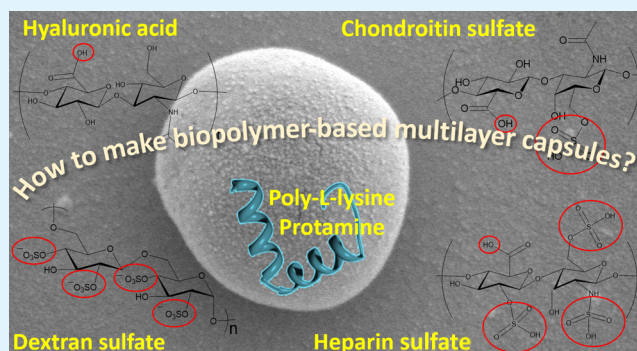Cite This: *ACS Appl. Mater. Interfaces* 2021, 13, 3259–3269

Read Online

ACCESS | 📊 Metrics & More | 📄 Article Recommendations | Ⓢ Supporting Information

ABSTRACT: The polymer layer-by-layer assembly is accounted among the most attractive approaches for the design of advanced drug delivery platforms and biomimetic materials in 2D and 3D. The multilayer capsules can be made of synthetic or biologically relevant (*e.g.*, natural) polymers. The biopolymers are advantageous for bioapplications; however, the design of such "biocapsules" is more challengeable due to intrinsic complexity and lability of biopolymers. Until now, there are no systematic studies that report the formation mechanism for multilayer biocapsules templated upon CaCO$_3$ crystals. This work evaluates the structure−property relationship for 16 types of capsules made of different biopolymers and proposes the capsule formation mechanism. The capsules have been fabricated upon mesoporous cores of vaterite CaCO$_3$, which served as a sacrificial template. Stable capsules of polycations poly-L-lysine or protamine and four different polyanions were successfully formed. However, capsules made using the polycation collagen and dextran amine underwent dissolution. Formation of the capsules has been correlated with the stability of the respective polyelectrolyte complexes at increased ionic strength. All formed capsules shrink upon core dissolution and the degree of shrinkage increased in the series of polyanions: heparin sulfate < dextran sulfate < chondroitin sulfate < hyaluronic acid. The same trend is observed for capsule adhesiveness to the glass surface, which correlates with the decrease in polymer charge density. The biopolymer length and charge density govern the capsule stability and internal structure; all formed biocapsules are of a matrix-type, other words are microgels. These findings can be translated to other biopolymers to predict biocapsule properties.

KEYWORDS: *multilayer, polyelectrolyte, calcium carbonate, vaterite, hard templating, sacrificial*
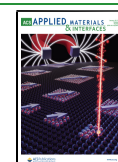
1. INTRODUCTION

In the past decades, a number of novel drug formulation strategies have emerged to enhance the therapeutic efficiency of the drugs.[1,2] Among others, polymer nano- and microcapsules are highlighted as especially promising candidates for this purpose. The advantages of polymer capsules comprise not only efficient drug entrapment[3−5] but also controlled drug release in response to physical−chemical triggers, which can be provided either by external stimuli[6−10] or by the internal microenvironment of the living tissue itself (*e.g.*, pH and temperature).[11,12] Besides this, diverse modifications of the capsule surface allow targeting toward specific cells.[3] Polymer capsules are conventionally fabricated using the layer-by-layer (LbL) assembly of polymers onto sacrificial templates, such as polymeric microgels or inorganic crystals, followed by the decomposition of these cores.[3−5] Since polyelectrolyte multilayers (PEMs) formed of biogenic polyelectrolytes are relatively nontoxic and biodegradable[13,14] and may possess specific bioactivities (*e.g.*, osteogenic[15] or anti-inflammatory[16]), there is a high demand for the design of biopolymer-based capsules.

Mesoporous crystals of carbonates have become the most popular sacrificial templates for LbL deposition due to their biocompatibility, nontoxicity, and highly developed internal structure that serves as an ideal network for the payload, as well as low cost and scalability.[17] Vaterite is one of the three polymorphs of calcium carbonate particles; vaterite crystals consist of porous nanodomains and hold high porosities.[18] The porosity, size, and the shape of the crystals can be widely tuned.[19−21] Importantly, vaterite crystals can be saturated with enormous amounts of macromolecules,[22] while the crystals grown in the presence of polymer matrices can host high amounts of small drugs.[23] Mild and nonharmful conditions of the decomposition of CaCO$_3$ cores make these templates

highly attractive for the use in a plethora of biomedical applications.[14,24−26]

Several studies have reported the templating of biopolymer-based capsules on vaterite cores. For instance, microcapsules made of poly-arginine (pARG) and heparin sulfate (HS);[27] pARG and dextran sulfate (DS);[28] DS and protamine (PR);[29] hyaluronic acid (HA) and poly-L-lysine (PLL);[30] and HA and collagen (COL)[31] have been templated upon pure vaterite CaCO₃ crystals. In alternate studies, the vaterite cores have been impregnated with a polymer matrix prior to LbL deposition in order to enhance the attraction of biopolymer layers. For example, chondroitin sulfate (CS)/PR and DS/PR capsules have been templated on polystyrene sulfonate-doped vaterite crystals.[32,33]

Alternatively, silica particles can also be used for the LbL deposition of biopolymers. This template is less common when compared with carbonates; a few biological examples include DS/chitosan[34] and HS/PR[35] capsules. In contrast to vaterite-templated capsules, silica-based capsules are hollow. Silica-templated capsules undergo little-to-moderate shrinkage after core dissolution with HF and may need a cross-linking agent to prevent the spontaneous release of the payload. They have been shown to be nontoxic and effective for drug delivery *in vivo*;[34,35] however, their main drawback is the need to use HF as a dissolution agent. Organic particles, such as colloidal polystyrene spheres, have been seen in many studies and are among those which have provided fundamental understanding of the LbL process and subsequent formation of both hybrid polymer/nanoparticle and pure polymer hollow shells.[36,37] These particles, however, require thermal treatment[37] or an organic solvent[38] to induce core decomposition/dissolution, which is damaging to biogenic polymer-based capsules.

Apart from inorganic particles, soft polymer microgels can also be utilized as sacrificial templates for LbL assembly.[39] These cores are prone to enzymatic degradation, which is used for their elimination and formation of such multilayer capsules. The behavior of PEM capsules upon degradation of the microgel core has been found to be strongly dependent on the biopolyelectrolytes used, for example, DS/pARG capsules remain intact and hollow after core degradation, while CS/pARG capsules rapidly rupture, which could be useful for pulsed drug delivery.[39]

It is worth to note that besides sacrificial templates, LbL coating has also been successfully applied for nonsacrificial cores, the most relevant examples of which are drug nanocores[40−42] and halloysite nanotubes.[43] The fundamental difference of these assemblies from capsule systems is in the retention of nonsacrificial cores with no need to dissolve them prior to the application.

Individual examples of the successful formulation of multilayer capsules constituting different biopolymer pairs that appear in the literature show high promise of these bioinspired capsules and their advantages over synthetic analogues. However, systematic evaluation of capsules made of different biopolymers remains absent. Single reports compare the structure and mechanical properties of synthetic- and biopolymer-based capsules,[30] but no studies compare capsules templated on sacrificial crystals made of different biopolymers. Meanwhile, this should be an important milestone in further development of biopolymer-based capsules. In this work, we have assembled 16 types of capsules made of different biopolymers utilizing vaterite CaCO₃ microcrystals as sacrificial cores. Stability of the capsules has been correlated with the stability of molecular polyelectrolyte complexes (PECs) formed between the biopolymers in solution in the absence of the CaCO₃ template. The comparative analysis of the capsule stability and internal structure helped to identify polyelectrolyte pairs with the highest potential for drug delivery and other biomedical applications.

2. EXPERIMENTAL SECTION

2.1. Materials. Calcium chloride dihydrate (Acros Organics, 10158280), sodium carbonate (Acros Organics, 10577182), sodium chloride (Fisher BioReagents, 10316943), EDTA [ethylenediaminete-traacetic acid (Fischer Scientific, 10335460)], chondroitin sulfate A 50 kDa (Creative PEGWorks, CS-114), fluorescein isothiocyanate–dextran sulfate sodium salt 40 kDa (Sigma, 51923), hyaluronic acid 50 kDa (Creative PEGWorks, HA-102), heparin sodium salt from porcine intestinal mucosa 10−12 kDa (Sigma, H5515), collagen type1 from rat tail 115−130 and 215−235 kDa (Sigma, 08−115), dextran amine 70 kDa (Creative PEGWorks DE-664), poly-L-lysine hydro-bromide 15−30 kDa and 150−300 kDa (Sigma-Aldrich, P7890 and P1399), protamine from salmon (Grade IV) 5−10 kDa (Sigma, P4005), fluorescein isothiocyanate-hyaluronic acid 50 kDa (Creative PEGWorks), fluorescein isothiocyanate-chondroitin sulfate A 50 kDa (Creative PEGWorks), fluorescein isothiocyanate isomer I was also from Sigma, and ethanol (absolute, >99%) was purchased from Fisher. Tris-buffered saline (10× Tris) pH 7.4 (Alfa Aesar, J60764) containing 250 mM Tris, 1.37 M sodium chloride, and 27 mM potassium chloride has been used. The water used in the experiments was prepared using a Millipore Milli-Q purification system and had a resistivity higher than 18.2 M Ω cm.

2.1.1. Synthesis of Calcium Carbonate. 100 mL of 50 mM CaCl₂ in 2× Tris was added to a glass beaker; the solution was then agitated at 650 rpm using a magnetic stirrer, followed by the addition of 100 mL of 50 mM Na₂CO₃ and further agitation for 60 s. The mixture was transferred from the beaker for crystal growth for 20 min. The crystals were then thoroughly washed twice with water (the crystal suspension was centrifuged at 1100*g* for 3 min), followed by the removal of the supernatant and the resuspension of the crystals in water. The crystals have been placed in a glass Petri dish and dried for 1 h at 70 °C.

2.1.2. Formation of Multilayer Capsules. The prepared crystals (4 mg/mL suspension) were alternately incubated in a polymer present in the 0.2× Tris buffer solution (5 mM Tris, 27.4 mM NaCl, and 0.54 mM KCl, with an additional 10 mM CaCl₂). For the deposition of the first layer, the crystals were suspended in 0.5 mL of the 0.2× Tris buffer solution, followed by the addition of 1.0 mL of the 0.5 mg/mL polymer in 0.2× Tris buffer. The suspension was then incubated on a shaker for 10 min at ca 1225 rpm to avoid sedimentation. The suspension was then centrifuged at 700*g* for 4 min; the supernatant was removed, followed by resuspension in 1.0 mL of the 0.2× Tris buffer solution and a second centrifugal step under the same conditions. The supernatant was then removed, and the coated crystals were then resuspended in 0.5 mL of the 0.2× Tris buffer solution, followed by a transfer to a new Eppendorf tube. The same steps were then applied for the next polyelectrolyte and repeated until the desired number of layers is achieved. The final pH value of the 0.2× Tris buffer solution was 7.9. Once the desired number of layers is achieved, the multilayer-coated crystals were suspended in 0.5 mL of the 0.2× Tris buffer solution. For the formation of multilayer capsules, 10 μL of the multilayer-coated crystal suspension was placed on a glass slide, with polystyrene-, ibidi-hydrophobic-, or ibidi-hydrophilic-coated wells (for the adherence experiments), followed by the addition of 10 μL of 50 mM EDTA. The remaining EDTA may be washed away *via* gentle pipetting using the same 0.2× Tris buffer solution. The multilayer-coated crystals were then frozen at −20 °C; the storage of the multilayer-coated crystals did not influence the results obtained in this study.

2.1.3. Turbidimetric Titration of the PECs with NaCl. Polymers have been dissolved in the 0.2× Tris buffer solution pH 7.9. PECs have been formed by the rapid addition of 0.4 mL of polycations to 0.4 mL of polyanions under continuous vigorous shaking for 30 s. The

mass concentration of polyanions in the PEC has been kept at 0.25 mg/mL (initial concentration of 0.5 mg/mL), while concentrations of polycations (except of the COL) have been chosen to keep the 1:1 M ratio between charged and uncharged groups of polyelectrolytes (recalculated per molecular unit). The 1:1 mass ratio has been chosen for COL due to complexity of the COL molecular structure. The 2 M solution of NaCl has been added to PECs by 20 μL drops until the total volume of 1.2 mL has been reached (equivalent of 400 μL of added 2 M NaCl). The absorbance has been recorded using a UV−vis spectrometer at a wavelength of 600 nm.

2.1.4. Conjugation of PLL with FITC. PLL has been conjugated with FITC in a theoretical molar ratio of 1:100 (FITC/monomer unit). The labeling reaction has been performed using 5.0 mg/mL polymers dissolved in the 0.1 M carbonate buffer solution (pH 9.0). The FITC solution was added dropwise to the polymer solution under constant stirring and left to incubate for 4 h at room temperature, kept out of the light. The resulting mixture was dialyzed with water repeatedly to separate the unreacted FITC; this was done using 3−5 kDa dialysis tubing.

2.1.5. Determination of the Capsule Shrinkage Coefficient. The shrinkage coefficient is the factor by which the final capsule diameter differs from that of the diameter of the multilayer-coated CaCO$_3$ crystal and is determined via the diving crystal diameter by the capsule diameter.

2.2. Characterization. *2.2.1. Dynamic Light Scattering.* Hydrodynamic diameters of both polysaccharides and proteins were determined using 1 mg/mL solutions in the 0.2× Tris buffer solution using ZetasizerNano ZS, Malvern, UK. The values were determined using a scattering angle of 173°. The final values were reported as intensity-, volume-, and number-weighted size distribution over three replicates.

2.2.2. Thermal Gravimetric Analysis. Thermal gravimetric analysis (TGA) was performed for the pure powdered polymer heated from 30 to 300 °C at a heating rate of 10 °C min^{-1} in a helium atmosphere using a TGA 4000 thermogravimetric analyzer, PerkinElmer, USA.

2.2.3. Fluorescence and Confocal Laser Scanning Microscopy. The Life Technologies EVOS FL microscope with 40× lens (USA) was used for routine analysis of the synthesized CaCO$_3$ crystals and capsules. Imaging was performed in both transmission and fluorescence modes. A confocal microscope TCS SP5 (Leica, Germany) was used for rigorous evaluation of the capsule structure. It was operated using a 488 nm excitation laser line. The images were processed using ImageJ 1.48V Software (Wayne Rasband, NIH, USA) to enhance brightness and color and to take fluorescence profiles.

2.2.4. Scanning Electron Microscopy. CaCO$_3$ crystal samples were prepared *via* depositing the dried powder onto carbon tape upon the aluminum sample stub to image their internal structure, and the crystals were cracked *via* mechanical force. Capsule samples were prepared *via* depositing 30 μL of coated-crystal suspension onto a circular glass slide, followed by the addition of 30 μL of 50 mM EDTA pH 7.0 for capsule formation (the same conditions for typical capsule preparation throughout the study). The resulting capsules were then washed with water repeatedly and frozen for freeze-drying. The slides with resulting freeze-dried capsules were sputtered with 10 nm of gold and imaged using the JSM-7100F field-emission scanning electron microscope (JEOL, USA). Both crystals and capsules were imaged using a probe current of 1 μA and an accelerating voltage of 2 kV.
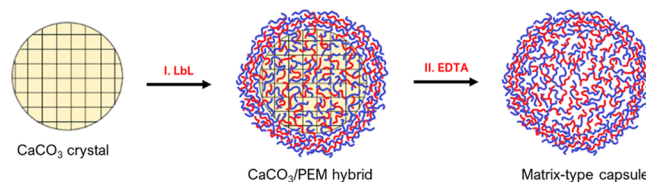
2.2.5. Energy-Dispersive X-ray Spectroscopy. The glass substrate, freeze-dried CaCO$_3$ crystals, and capsules deposited upon the glass substrate (sputtered with 10 nm of gold) were subjected to energy-dispersive X-ray spectroscopy (EDX) analysis, operated at a probe current of 10 μA and an accelerating voltage of 10 kV.

3. RESULTS AND DISCUSSION

In this study, porous vaterite CaCO$_3$ microcrystals have been utilized as sacrificial templates for capsule formation. The use of vaterite as a capsule template can give rise to two types of capsule structures, either a hollow or matrix type. Hollow capsules are those composed of a multilayer capsule shell and a hollow lumen, while a matrix-type capsule consists of an internal polymer matrix, which results from the permeation of the polyelectrolytes into the pores of the crystal during the deposition process.[44] Coating of the crystals with PEMs constituting different biopolyelectrolytes [Scheme 1(I)] was

Scheme 1. Schematic of LbL Capsule Fabrication on Vaterite Calcium Carbonate Cores: (I) LbL Deposition of PEMs on CaCO$_3$ Crystals Resulting in Partial Penetration of the Polymers inside the Crystal Pores and Formation of the PEM Shell on the Crystal Surface and (II) elimination of CaCO$_3$ Crystals by the Addition of a Chelating Agent (EDTA) Resulting in the Formation of Matrix-Type Capsules
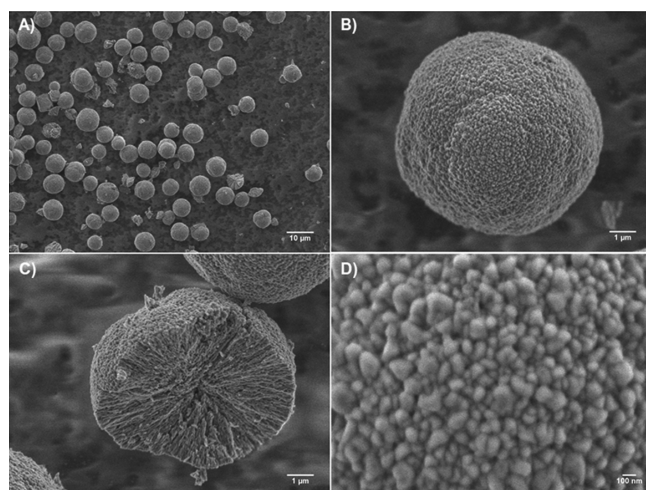

followed by core elimination with EDTA that resulted in the formation of matrix-type multilayer capsules [Scheme 1(II)]. This approach has been chosen as the conventional and most common procedure for the fabrication of LbL capsules.[45]

3.1. Vaterite Cores. Vaterite microcrystals have been prepared according to the protocol described in previous works,[46] with some modifications. Recent reports revealed that the substitution of conventionally used water with buffered solutions is important for the preservation of bioactivity of some biomolecules while having no pronounced effect on the crystal structure.[47] For instance, there is the problem of potential irreversible conformational changes at pHs above 9, as shown during the loading of catalase into such vaterite cores,[47] while pHs below 7 are not suitable for the LbL coating of CaCO$_3$ crystals due to their dissolution. Bearing the protection of such macromolecular drugs in mind, the pH was maintained at 7.9 throughout all the experiments in this study.

In full accordance with literature data, the crystals were of a spherical shape and mesoporous in structure, which have been confirmed by scanning electron microscopy (SEM) (Figure 1). The content of calcite was below 5%; the total mass yield of CaCO$_3$ exceeded 95%. The size of the crystals was 9 ± 3 μm without significant differences between batches of synthesized crystals. Mechanically broken crystals (Figure 1C) bare narrow and interconnected cylindrical pores formed by nanocrystallines. The size of nanocrystallites at the crystal surface calculated from SEM (typical image is presented in Figure 1D) was 138 ± 22 nm, of the same order as previously reported for crystals prepared in water.[46,48]

3.2. Biopolyelectrolytes in Solution. Polyelectrolytes chosen for this study comprised four polycations and four polyanions (Figure 2). Polyelectrolytes that generate anions were of either solely carboxylic (HA) and solely sulfuric (DS) nature or contained both COO$^-$ and sulfate groups in ratios 1:1 and 1:3 (for CS and HS, respectively). The four polycations used generated amino groups and had different conformations and structures, that is, two proteins—fibrous COL and globular PR and two linear polymers—highly charged PLL and DA, which carry a lower net charge.

Figure 1. Representative SEM images of CaCO$_3$ crystals: (A) overview of crystals, (B) single crystal, (C) cross-section of the mechanically broken crystal, and (D) surface morphology of the crystal.
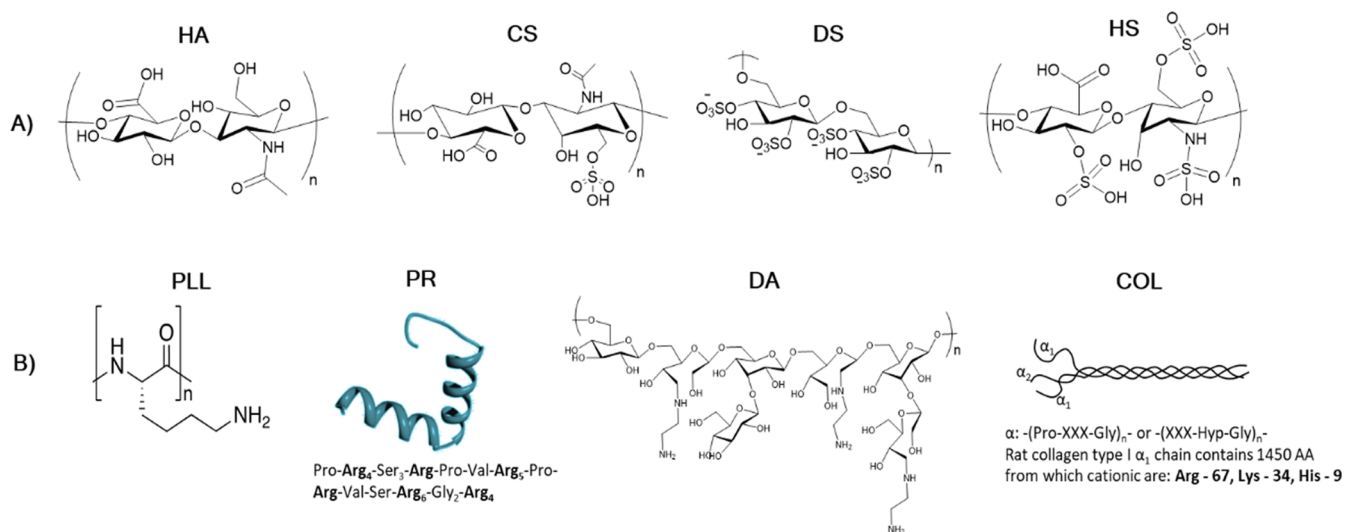
Table S1 displays the respective pK_a and isoelectric points of polymers and proteins, respectively. Hydrodynamic radii (R_h) of these polymers in the Tris buffer solution pH 7.9 were determined by dynamic light scattering (DLS). Figure 3 presents their size distributions by volume fractions (see Figure S1 for intensity- and number-weighted distributions). DLS data suggest that polyanions were of a similar size, that is, R_h in the range of 3−4 nm for CS, DS, and HS and slightly more (7.2 ± 3.4 nm) for HA. In contrast, R_h of polycations significantly increased in the series PR ≃ PLL < COL < DA ranging from a few nanometers for PR and PLL, 107 ± 14 nm for COL, and up to a few micrometers for DA. Notably, only DA is prone to aggregation and predominantly forms microsized clusters in the Tris buffer solution pH 7.9. Other polymers were present in a nonaggregated state.

3.3. Formation of Biopolymer-Based Capsules. CaCO$_3$ crystals have been coated with (polyanion/polycation)$_2$-polyanion multilayers made of 16 combinations of these

polymers. During the coating and capsule formation processes, the temperature remained standard; it is reasonable to assume that the increase of temperature, for example, to a physiological value of 37 °C, may promote enhanced polyelectrolyte adsorption and the formation of a thicker multilayer shell, in accordance with modern LbL concepts. This, in turn, may significantly affect the structure and functionality of the final capsules.

Elimination of the cores was induced by the addition of EDTA, which caused the dissolution of CaCO$_3$ crystals and either the formation of the capsules or disintegration of the multilayer shells (Figure S2). Under these conditions, none of the DA- and COL-based capsules coupled with HA, CS, DS, or HS; all DA- and COL-based coatings underwent complete dissolution upon the elimination of the cores. However, 8 out of 16 probed biopolymer pairs, that is, PLL-based (HA/PLL, CS/PLL, DS/PLL, and HS/PLL) and PR-based (HA/PR, CS/PR, DS/PR, and HS/PR), formed stable capsules.

Comparison of these results with literature data is summarized in Table 1. While some of the pairs have been reported here for the first time (HA/PR; HS/PR; HS/PLL; and DS/PLL), other biogenic polyelectrolyte pairs were used for the fabrication of CaCO$_3$-templated capsules in recent reports. Thus, multilayer CS/PLL[50] and CS/PR[32] capsules were templated on vaterite microcrystals. In contrast to our study, the microcrystals were preloaded with polyanionic CS[50] or PSS[32] *via* cosynthesis. CS/PLL capsules were not stable, and this instability was solved *via* capsule cross-linking.[50] Besides this, the capsules formed by CS and another polyamino acid, pARG, were reported.[51] Similarly, CaCO$_3$-templated HS/pARG and DS/pARG capsules were investigated in a few studies;[13,27,28] successful fabrication of CS/pARG and DS/pARG capsules from soft microtemplates is also reported.[39] Fabrication of DS/PR capsules has also been attempted but faced either the problem of capsule aggregation when DS was a capping layer[29] or significant (up to 40%) retention of CaCO$_3$ after core dissolution when CaCO$_3$ was doped with PSS.[33] It is important to note that the problem of colloidal stability is often reported for LbL deposition on the cores of various nature.[52]

Figure 2. Structure of polymers utilized in this study separated into two categories: (A) polyanionic and (B) polycationic. For the proteins, the amino acid sequence (for PR) or the number of positively charged amino acids (Arg, Lys, and His) per α_1-helix (for COL) is given. The PR structure is adapted with the permission.[49]
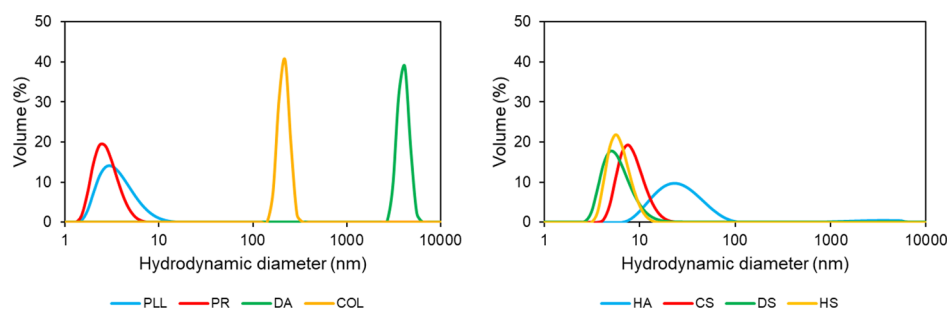
Figure 3. DLS size distribution of polyanions and polycations in the Tris buffer solution (1 mg/mL).

Table 1. Comparison of CaCO$_3$-Templated Multilayer Capsules Made of Different Biopolyelectrolytes and Fabricated in This Study with Literature Data^a

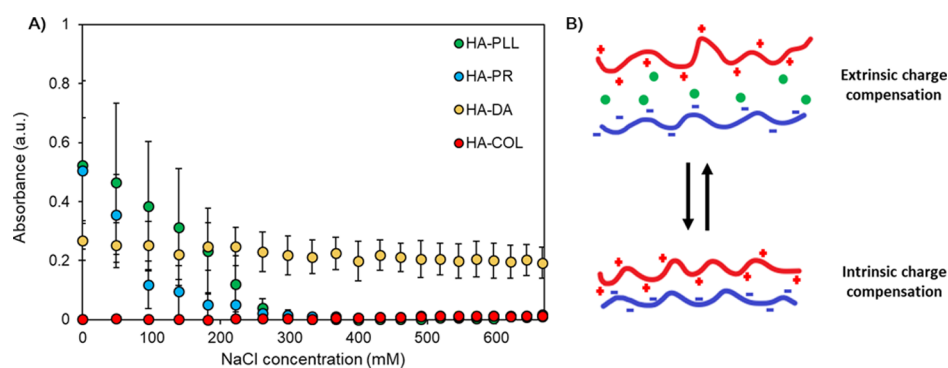| polycation | polyanion | | | | | | | |
| | HA | | CS | | DS | | HS | |
	formed in this study?	Lit.	formed in this study?	Lit.	formed in this study?	Lit.	formed in this study?	Lit.
PLL	yes	not suitable due to high shrinkage[30]	yes	CaCO$_3$-CS cores; capsules not stable[50]	yes	NR	yes	NR
PR	yes	NR	yes	CaCO$_3$-PSS cores[32]	yes	-Heavily aggregated capsules[29] -CaCO$_3$-PSS cores, CaCO$_3$ retains in the capsule[33]	yes	NR
DA	no	NR	no	NR	no	NR	no	NR
COL	no	fabricated using cross-linked COL[31]	no	NR	no	NR	no	NR

^{a}NR—not reported.

Figure 4. (A) Turbidimetric titration of PECs of HA and PLL, PR, COL, or DA and formed in the Tris buffer solution pH 7.9. The initial concentration of NaCl is subtracted; the x-axis represents the added amount of NaCl. (B) Schematic of intrinsic and extrinsic charge compensation within multilayers. The pluses, minuses, and green circles represent permanent positive charges, permanent negative charges, and counterions, respectively.
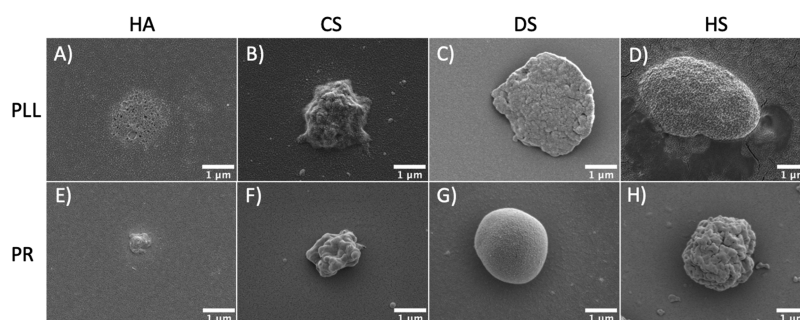
Interestingly, although HA/PLL capsules were reported, they did not receive proper attention due to a high degree of capsule shrinkage during their preparation.[30] However, we strongly believe that such a behavior may be beneficial for drug delivery purposes as a way to intrinsically reduce the capsule size and entrap molecules of interest. Notably, fabrication of HA/COL capsules utilizing cross-linked COL was also reported.[31] It seems that the fabrication of COL-based capsules without chemical modifications cannot be achieved. This suggests that the integrity and stability of the capsules that underwent dissolution in our study can be improved *via* chemical modifications of the polymers and their cross-linking; however, this is out of the scope of this paper. Of note, for obvious reasons, we also exclude the consideration of capsules templated on nanocores such as drug nanocrystals or silica.

3.4. Probability of Capsule Formation versus PEC Stability. For this purpose, interactions of oppositely charged polymers in an aqueous environment have been probed by means of turbidimetric titration of equimolar complexes. PECs were formed in the Tris buffer solution pH 7.9, which had the same composition as the solution used for the fabrication of capsules. Then, PECs were titrated with salt (NaCl) until their dissolution. Figure 4A shows the turbidimetric curves obtained for the titration of PECs composed from HA and different polycations as an example. The ionic strength was increased stepwise until the critical concentration of NaCl (C_{crit}) was reached, at which point the PECs underwent dissolution due to the extensive screening of polyelectrolyte permanent charges by salt. It is expected that the higher the value of this C_{crit}, the more the ion pairs are formed between the polymer chains in the initial PECs (Figure 4B). Since the conditions used for the

Table 2. Shrinkage Coefficients and Adherence of PLL- and PR-Based Capsules[a]

polyanion	shrinkage coefficient		adherence after wash (%)		charged groups per polyanion monomer
	PLL	PR	PLL	PR	
HA	5.39 ± 1.34	7.09 ± 1.85	96.8 ± 2.5	95.4 ± 2.2	1.0
CS	2.72 ± 0.61	2.83 ± 0.64	98.1 ± 1.9	97.9 ± 1.2	2.0
DS	1.77 ± 0.42	2.30 ± 0.56	43.1 ± 16.4	92.9 ± 6.2	4.6
HS	1.33 ± 0.24	1.69 ± 0.30	0.0 ± 0.0	93.4 ± 2.2	5.2

[a]$CaCO_3$ cores have been dissolved by the addition of 50 mM EDTA. The diameter of coated crystals is 7.5 ± 0.8 μm. Surface-adhering abilities of capsules are calculated after repeated washing steps with 5 mM Tris containing 27 mM NaCl, 10 mM $CaCl_2$ with pH 7.9, taking the initial number of capsules as 100%. Error bars are S.D. for at least n = 100 measurements.

Figure 5. Typical SEM images of 10 nm gold-sputtered capsules consisting of 2.5 bilayers. PLL-based (top row) capsules consisting of HA, CS, DS, and HS are shown in images (A), (B), (C), and (D), respectively. PR-based (bottom row) capsules, consisting of HA, CS, DS, and HS, are shown in images (E), (F), (G), and (H), respectively. Scale bars are 1 μm.

formation of PECs and corresponding capsules are the same, in its turn, the higher C_{crit} should correspond to stronger capsule integrity. Indeed, the results of the turbidimetric titration of PECs correlate with the probability of capsule formation upon core dissolution. As follows from turbidimetric titrations, HA is not prone to forming strong PECs with COL and DA in solution. Of note, slight turbidity of HA/DA is most likely associated with the formation of DA aggregates in the buffer solution (Figure 3). Weak complexation with COL is likely due to its low pI value (Table S1). In contrast, PR and PLL form complexes that dissolve due to extrinsic charge compensation at $C_{crit} \approx 300$ mM. This correlates with their high pI/pK_a value (Table S1). Other PECs behaved similarly (Figure S3 for CS/polycation PECs); this allowed us to correlate the formation of the capsules and the formation of PECs in solution.
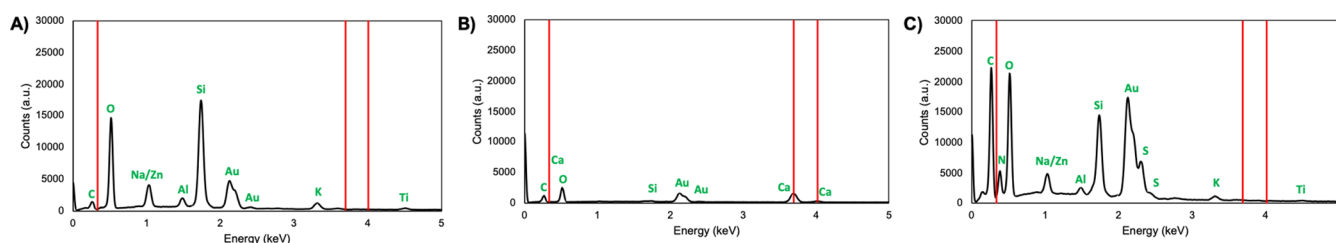
3.5. Shrinkage and Adherence of the Capsules. It is notable that the elimination of the vaterite core triggered reorganization of the polymer matrices, resulting in the reduction of capsule sizes. The degree of shrinkage was dependent on the type of the polymer used (Table 2). There was no direct correlation between the degree of shrinkage and the results of the turbidimetric titration (C_{crit}). Moreover, there was no direct correlation between the degree of polymer hydration and the shrinkage of the capsules. During TGA, all the biopolymers that form stable capsules lost ca. 7−20% in weight from thermic dehydration (Figure S4). However, a clear trend of increasing degrees of shrinkage was observed following a series of DS ≈ HS < CS < HA. Interestingly, it can be correlated with the increasing number of charged groups per polyanion monomer (Table 2). It is of note that, in the literature, multiple synthetic polyelectrolyte-based capsules have been formed and exhibit shrinkage behavior too. The approaches used to induce shrinkage appear to be analogous to that of biopolymer-based capsules formed here and in the literature. For instance, the variation of ionic strength has been shown to induce shrinkage in both poly(styrenesulfonate)

(PSS)/poly(diallyldimethylammonium chloride) (PDAD-MAC)[53] and PSS/poly(allylamine hydrochloride)[54] capsules, while temperature-induced shrinkage has been demonstrated in PSS/PDADMAC,[12,55] PSS/PAH,[56] and in the biologically relevant DS/pARG system.[57]
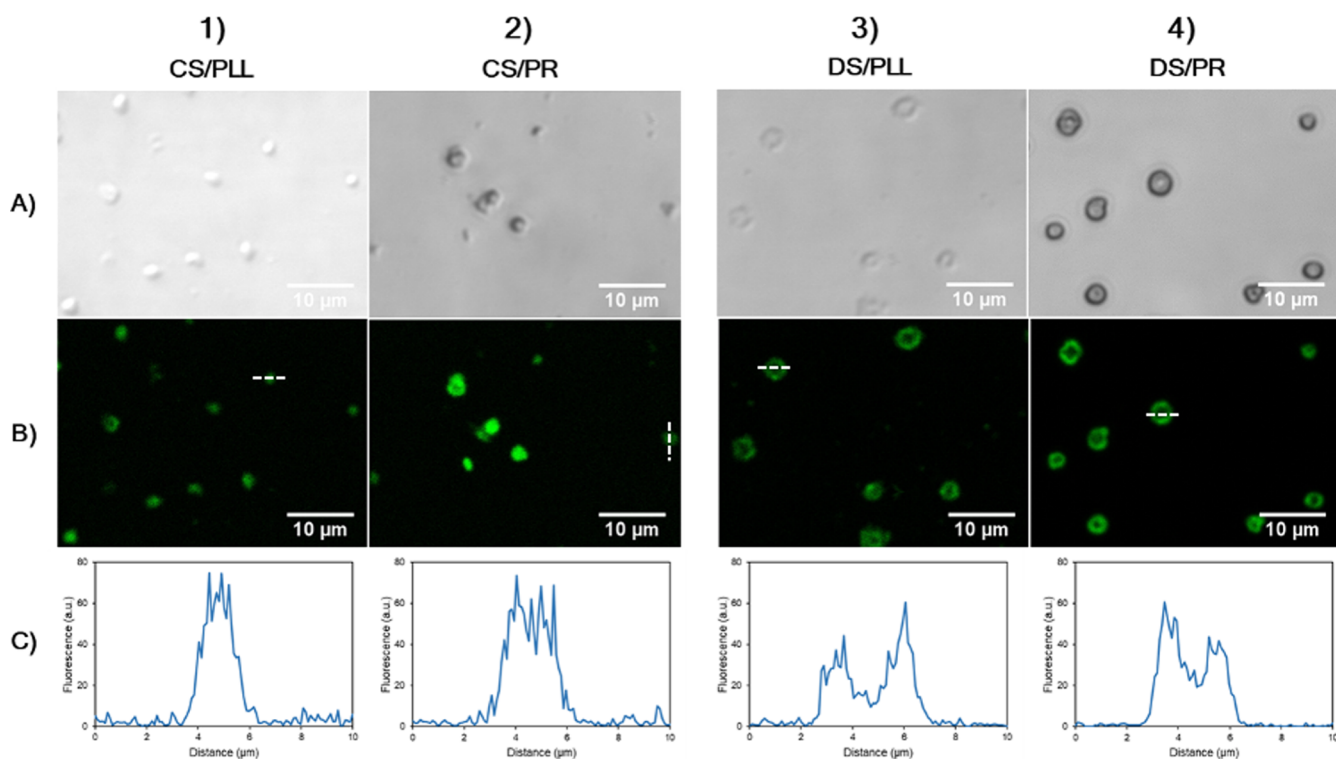
At the same time, despite the lower charge density, PR-based capsules are prone to a higher degree of shrinkage than PLL-based capsules. This may be associated with lower diffusivity and the larger number of polyion contacts of highly charged PLL with the polyanions, which leads to the reduced and slower PLL molecular and chain dynamics during the elimination of the core and consequently results in a lower degree of shrinkage.

These data correlate with the adherence of capsules to the glass surface, which has been assessed via optical microscopy of the capsules before and after repeated washing steps with the Tris buffer solution (Figure S5, Table 2). It is reasonable to assume that the high adherence of PR-based capsules to the hydrophilic glass surface (of which is negatively charged with silanol groups) is due to a large number of free non-compensated charges of PR on the outer surface of the capsules. In contrast, PLL has a larger number of contacts with the polyanions and a lower number of charged free amino groups. As a result, adherence of PLL-based capsules to the glass surface is lower if compared to that of PR-based ones. The choice of polyanions does not affect the adherence of PR-based capsules; however, it has a pronounced effect on the adherence of PLL-based capsules, which directly depends on the charge density of polyanions. Namely, the more charged groups per polyanion monomer, the fewer the noncompensated amino groups of PLL and, accordingly, the less the adherence of the capsules.

In order to better understand the adherence mechanism, PLL- and PR-based capsules have also been prepared on the surfaces of other types: polystyrene-, ibidi-hydrophobic- and ibidi-hydrophilic-coated wells (Figure S6). The type of the

Figure 6. Typical EDX spectra of the 10 nm gold-sputtered (A) glass substrate, (B) bare $CaCO_3$ crystals, and (C) $(DS/PR)_{2.5}$ capsules. The red lines correspond to the characteristic energies of X-ray emission for calcium, as subject to the $CaCO_3$ crystal controls.

Figure 7. Confocal images of (1) $(CS^{FITC}/PLL)_{2.5}$, (2) $(CS^{FITC}/PR)_{2.5}$, (3) $(DS^{FITC}/PLL)_{2.5}$, and (4) $(DS^{FITC}/PR)_{2.5}$ capsules. (A) Bright field, (B) fluorescence (excitation at 488 nm) images of capsules, and (C) corresponding linear fluorescence profiles taken across the middle of the capsules. Capsules are prepared on $CaCO_3$ cores of $9 \pm 3 \, \mu$m in diameter. $CaCO_3$ cores have been dissolved by the addition of 50 mM EDTA. The white dashed lines indicate how the line profiles were taken.

surface coating did not affect the adherence of neither PLL- nor PR-based capsules that might indicate the pivotal role of the hydrophobicity of the capsules on their adhesiveness. This is also supported by the decrease of the adhesiveness of PLL-based capsules with the decrease of their shrinkage coefficient and, consequently, increase of their water content. However, no similar trend was observed for PR-based capsules: their adherence was close to 100% even for the PR/HS biopolyelectrolyte pair and no correlation between capsule adhesiveness and degree of capsule shrinkage has been found (Table 2, Figure S6). This might be associated with the globular structure, compact size, and protein nature of the PR that probably undergoes conformational changes upon interaction with polyanions and upon capsule adsorption on the surfaces, which brings new types of interactions into the system. Similar conformational changes have been previously reported for the LbL of large proteins on polystyrene beads.[58] In addition, the capsules formed by DS demonstrated significantly lower adherence to polystyrene coating than to other substrates and compared to other polyelectrolytes. These

findings might be important for different applications such as micropatterning of the surfaces and decoration of the implants with functional microcapsules. Further studies should shed more light on the adherence mechanism.

3.6. Internal Structure of the Capsules. Successfully fabricated capsules were lyophilized and visualized by SEM (Figure 5). The complete elimination of $CaCO_3$ cores was confirmed by EDX analysis (Figure 6). Apart from the glass substrate and coating material elements (Figure 6A), EDX spectra of $CaCO_3$ contain characteristic energy bands of Ca (Figure 6B). These bands are not found in the spectra of the capsules (Figure 6C). Similarly, the complete elimination of calcium carbonate has been proven for all other types of capsules (data are not shown). Depending on the degree of shrinkage, the final capsules are of different sizes, but they all maintain a clear spherical structure and are filled with a polymer matrix, resulting in the formation of microgels rather than classical hollow structures (Figures 5 and S7). This may be important for capsule stabilization during core dissolution and for their further performance of drug encapsulation and

release. A deeper investigation is necessary to further probe the capsule internal structure *via* use of advanced approaches including small-angle X-ray scattering analysis[59] and confirm the presence of such a polymer matrix within the capsules.

Polymer distribution inside the capsules has been investigated by means of confocal laser scanning microscopy (CLSM) imaging of the crystals coated with (polyanion^{FITC}/polycation)$_2$-polyanion before the elimination of CaCO$_3$ and the imaging of corresponding multilayer capsules. Figure S8 shows the uniform and homogeneous distribution of FITC polymers within the entire internal volume of mesoporous vaterite crystals. CLSM imaging of the capsules (Figure 7) revealed that the polymers remain in the capsule lumen after the dissolution of the core and therefore occupy the interior of the capsule instead of forming a thin shell. Such a matrix-type structure was common for all types of the capsules probed in this study; however, the degree of the capsule "filling" with a polyelectrolyte differed for the capsules of different compositions. Namely, it seems to decrease in a series of HA > CS > DS > HS (as illustrated in Figure S9 for PLL-based capsules). However, we suppose that this is an artificial trend that cannot be reliably attributed to the nature of biopolymers used. The possible reason for the observed difference in the capsule "filling" is the insufficient resolution for smaller HA/PLL and CS/PLL capsules, which does not allow us to probe their internal structure accurately. These possible optical effects restrict us from the deeper analysis of capsule "filling" dependencies on the polymer composition.
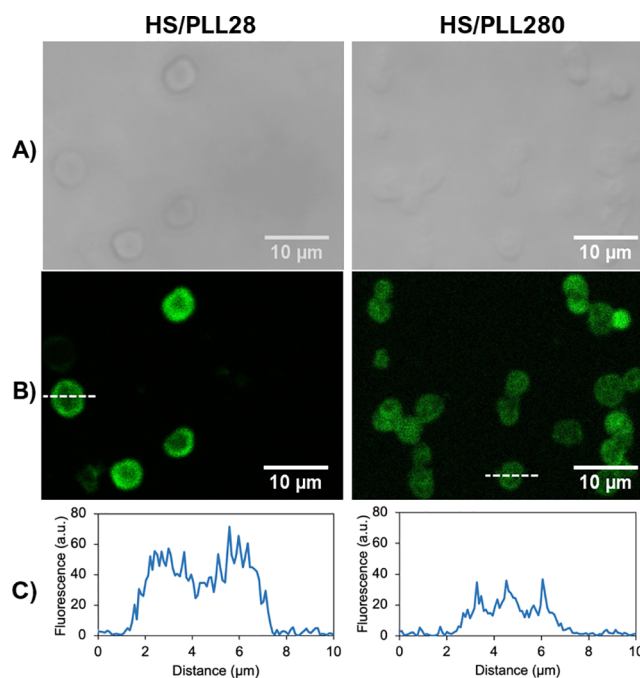
It is worth noting that in the literature, biopolymer-based capsules prepared under similar conditions were more often denoted as hollow-type capsules.[27,31,51] We assume, to a large extent, that this is a question of terminology and should be considered with care. For example, Figure 7 shows that DS-based capsules maintain their core–shell structure; however, they still have a polymer matrix in the capsule interior. In this particular case, the presence of the polymer matrix is obvious and cannot be neglected, and therefore, the capsules cannot be denoted as hollow. However, if the capsules contain less polymers inside, the presence of the polymer matrix is often ignored due to its insignificance.[27] The question of establishing a proper threshold of the degree of polymer "filling" between matrix- and hollow-type capsules has been addressed in other studies.[44]

However, we would like to point toward the pronounced difference between PR- and PLL-based capsules that is clearly visible within the transmittance images (Figure 7). Although both are matrix-type, PR-based capsules have a denser structure evidenced by their higher absorbance of light. PLL capsules transmit light at a higher degree, which makes their images in an aqueous medium much less contrasting. This can indicate a lower water content of PR-based capsules, which correlates well with the higher adherence of these capsules (Table 2). Further investigation of this question requires more precise analysis of the capsule structure and is left for upcoming studies.

3.7. PLL$_{28}$- versus PLL$_{280}$-Based Capsules. Bearing in mind that the filling of the capsules with polymer matrices is important for their loading/release performance, next, we attempted to find a way to control the internal structure of these capsules and investigated the effect of the polymer length on the capsule shrinkage and internal structure. For this, capsules have been fabricated using PLL with two different median molecular weights of 28 and 280 kDa (denoted as PLL$_{28}$ and PLL$_{280}$, respectively), as previously determined by the HPLC system in a previous study.[60] Hydrodynamic diameters of PLL$_{28}$ and PLL$_{280}$ in the Tris buffer solution pH 7.9 have been measured by DLS and found to be 3.9 ± 1.9 and 15.6 ± 7.6 nm, respectively. Both polymers have been conjugated with FITC for the probing of their distribution inside the capsules by means of CLSM imaging.

This suggests that the PLL length makes little difference to the internal structure of capsules when the polyanion remains constant. Figure 8 shows confocal images of HS/PLL$_{28}$ and
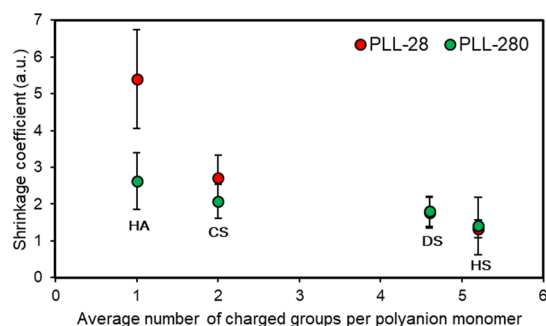

Figure 8. Confocal images of HS/PLL$_{28}^{FITC}$ and HS/PLL$_{280}^{FITC}$ capsules: (A) bright field, (B) fluorescence (excitation at 488 nm) images of capsules, and (C) corresponding linear fluorescence profiles taken across the center of the capsules. Capsules are prepared on CaCO$_3$ cores of 7.5 ± 0.8 μm in diameter. The cores have been dissolved by the addition of 50 mM EDTA. The white dashed line indicates how the line profile was taken.

HS/PLL$_{280}$ capsules as a representative example. Despite the larger molecular size of PLL$_{280}$, its penetration into the large pores of vaterite crystals during polymer deposition leads to the formation of a polymer matrix, similar to that of smaller PLL$_{28}$, that is, both PLLs are evenly distributed throughout the entire volume of the capsules.

The shrinkage behavior of PLL$_{28}$- and PLL$_{280}$-based capsules has also been compared. It was found that, similar to PLL$_{28}$, the degree of the shrinkage of PLL$_{280}$-based capsules decreases with the increase of the number of charged groups on the polyanion. At the same time, increasing the PLL length significantly decreases the shrinkage coefficients of such systems (Figure 9). This effect is more pronounced for HA/PLL capsules, creating twice the difference in the shrinkage of these capsules. The lower degree of the shrinkage in PLL$_{280}$-based capsules may be attributed to lower diffusivity and dynamics of PLL$_{280}$ molecules, which results in reduced polymer reorganization during the dissolution of the core. This provides a simple approach to control the degree of capsule shrinkage, which is important for their utilization within biomedical applications.

Figure 9. Effect of the number of charged groups within the polyanion monomer unit upon the shrinkage coefficient of PLL_{28}- and PLL_{280}-based capsules. $CaCO_3$ cores have been dissolved by the addition of 50 mM EDTA. The diameter of coated crystals is 7.5 ± 0.8 μm. Error bars are S.D. for at least n = 100 measurements.

4. CONCLUSIONS

This paper presents a comparative study of 16 types of multilayer capsules made of biogenic polyelectrolytes templated upon vaterite $CaCO_3$ microcrystals. PLL and PR are able to form stable capsules with all tested anionic polymers and are prone to shrinkage upon core dissolution. The degree of shrinkage increased in a series of HS < DS < CS < HA, which correlates with the decrease in polymer charge density. Similarly, capsule adherence to the glass surface increases with the decrease in polyanion charge density due to a reduced internal compensation of charges within the multilayers. All tested COL- and DA-based capsules underwent dissolution during core elimination. Formation of the capsules has been correlated with the stability of polyelectrolyte complexes in solution. The internal structure of the capsules was investigated by means of confocal and scanning electron microscopies, revealing the presence of a polymer matrix inside the capsule lumen. The effect of the polymer molecular weight on the shrinkage and internal structure of capsules was verified using PLL of different lengths, which exhibit no influence on polymer distribution inside the capsule and a significant decrease of the shrinkage coefficients with increasing PLL length. Depending on the type of polycations (PR and PLL), their molecular weight, and the type of polyanions, it is possible to design biocapsules that would have certain properties and tailor them in accordance with desired applications in a broad range: from shrinkable (almost 2 orders of magnitude by volume) to nonshrinkable (shrinkage coefficient ≈ 1), from a hollow to matrix type, and from adhesive (adherence > 90%) to nonadhesive (adherence closed to 0) biocapsules. This study reveals clear dependencies of the biopolymer-based capsule formation, shrinkage, and internal structure on their polymer composition, which can be translated to other biopolyelectrolyte pairs; this is an important milestone in the further development of biopolymer-based capsules for drug delivery, tissue engineering, and other biomedical applications.

ASSOCIATED CONTENT

Ⓢ Supporting Information

The Supporting Information is available free of charge at https://pubs.acs.org/doi/10.1021/acsami.0c21194.

pK_a and pI data for polymers, intensity- and number-weighted distributions of polymers, transmittance and fluorescent images of initial capsule screening, turbidi-

metric titration curves for CS-based PECs, TGA curves of polymers used, and transmittance images of before and after washing stages with the Tris buffer (PDF)

AUTHOR INFORMATION

Corresponding Authors

Dmitry Volodkin − *Department of Chemistry and Forensics, School of Science and Technology, Nottingham Trent University, NG11 8NS Nottingham, U.K.;* ⓞ orcid.org/0000-0001-7474-5329; Phone: +44-115-848-3140; Email: dmitry.volodkin@ntu.ac.uk

Anna S. Vikulina − *Branch Bioanalytics and Bioprocesses, Fraunhofer Institute for Cell Therapy and Immunology, 14476 Potsdam, Germany;* ⓞ orcid.org/0000-0001-9427-2055; Phone: +49-331 58187-122; Email: anna.vikulina@izi-bb.fraunhofer.de

Authors

Jack Campbell − *Department of Chemistry and Forensics, School of Science and Technology, Nottingham Trent University, NG11 8NS Nottingham, U.K.*

Jordan Abnett − *Department of Chemistry and Forensics, School of Science and Technology, Nottingham Trent University, NG11 8NS Nottingham, U.K.*

Georgia Kastania − *Department of Chemistry and Forensics, School of Science and Technology, Nottingham Trent University, NG11 8NS Nottingham, U.K.*

Complete contact information is available at:
https://pubs.acs.org/10.1021/acsami.0c21194

Author Contributions

The manuscript was written through contributions of all authors. All authors have given approval to the final version of the manuscript.

Notes

The authors declare no competing financial interest.

ABBREVIATIONS

COL, collagen type 1
CS, chondroitin sulfate
DA, dextran amine
DS, dextran sulfate
HA, hyaluronic acid
HS, heparin sulfate
pARG, polyarginine
PLL, poly-L-lysine
PR, protamine
LbL, layer-by-layer
PEC, polyelectrolyte complex
PEMs, polyelectrolyte multilayers
pI, isoelectric point

■ REFERENCES

(1) Lombardo, D.; Kiselev, M. A.; Caccamo, M. T. Smart Nanoparticles for Drug Delivery Application: Development of Versatile Nanocarrier Platforms in Biotechnology and Nanomedicine. *J. Nanomater.* **2019**, *2019*, 3702518.

(2) Correa, S.; Dreaden, E. C.; Gu, L.; Hammond, P. T. Engineering Nanolayered Particles for Modular Drug Delivery. *J. Controlled Release* **2016**, *240*, 364−386.

(3) Del Mercato, L. L.; Ferraro, M. M.; Baldassarre, F.; Mancarella, S.; Greco, V.; Rinaldi, R.; Leporatti, S. Biological Applications of LbL Multilayer Capsules: From Drug Delivery to Sensing. *Adv. Colloid Interface Sci.* **2014**, *207*, 139−154.

(4) De Koker, S.; Hoogenboom, R.; De Geest, B. G. Polymeric Multilayer Capsules for Drug Delivery. *Chem. Soc. Rev.* **2012**, *41*, 2867−2884.

(5) Volodkin, D.; von Klitzing, R.; Moehwald, H. Polyelectrolyte Multilayers: Towards Single Cell Studies. *Polymers* **2014**, *6*, 1502−1527.

(6) Esser-Kahn, A. P.; Odom, S. A.; Sottos, N. R.; White, S. R.; Moore, J. S. Triggered Release from Polymer Capsules. *Macromolecules* **2011**, *44*, 5539−5553.

(7) Parakhonskiy, B. V.; Yashchenok, A. M.; Möhwald, H.; Volodkin, D.; Skirtach, A. G. Release from Polyelectrolyte Multilayer Capsules in Solution and on Polymeric Surfaces. *Adv. Mater. Interfaces* **2017**, *4*, 1600273.

(8) Parakhonskiy, B. V.; Parak, W. J.; Volodkin, D.; Skirtach, A. G. Hybrids of Polymeric Capsules, Lipids, and Nanoparticles: Thermodynamics and Temperature Rise at the Nanoscale and Emerging Applications. *Langmuir* **2019**, *35*, 8574−8583.

(9) Demina, P. A.; Voronin, D. V.; Lengert, E. V.; Abramova, A. M.; Atkin, V. S.; Nabatov, B. V.; Semenov, A. P.; Shchukin, D. G.; Bukreeva, T. V. Freezing-Induced Loading of TiO2 into Porous Vaterite Microparticles: Preparation of CaCO₃/TiO₂ Composites as Templates to Assemble UV-Responsive Microcapsules for Wastewater Treatment. *ACS Omega* **2020**, *5*, 4115−4124.

(10) Borodina, T.; Trushina, D.; Artemov, V.; Bukreeva, T.; Shchukin, D. Modification of the Polyelectrolyte Capsule Shell by Nanodiamonds for Remote Microwave Opening. *Mater. Lett.* **2019**, *251*, 81−84.

(11) Sato, K.; Yoshida, K.; Takahashi, S.; Anzai, J.-i. PH- and Sugar-Sensitive Layer-by-Layer Films and Microcapsules for Drug Delivery. *Adv. Drug Delivery Rev.* **2011**, *63*, 809−821.

(12) Van der Meeren, L.; Li, J.; Konrad, M.; Skirtach, A. G.; Volodkin, D.; Parakhonskiy, B. V. Temperature Window for Encapsulation of an Enzyme into Thermally Shrunk, CaCO₃ Templated Polyelectrolyte Multilayer Capsules. *Macromol. Biosci.* **2020**, *20*, 2000081.

(13) Trushina, D. B.; Akasov, R. A.; Khovankina, A. V.; Borodina, T. N.; Bukreeva, T. V.; Markvicheva, E. A. Doxorubicin-Loaded Biodegradable Capsules: Temperature Induced Shrinking and Study of Cytotoxicity in Vitro. *J. Mol. Liq.* **2019**, *284*, 215−224.

(14) Novoselova, M. V.; Loh, H. M.; Trushina, D. B.; Ketkar, A.; Abakumova, T. O.; Zatsepin, T. S.; Kakran, M.; Brzozowska, A. M.; Lau, H. H.; Gorin, D. A.; Antipina, M. N.; Brichkina, A. I. Biodegradable Polymeric Multilayer Capsules for Therapy of Lung Cancer. *ACS Appl. Mater. Interfaces* **2020**, *12*, 5610−5623.

(15) Guduru, D.; Niepel, M. S.; Gonzalez-Garcia, C.; Salmeron-Sanchez, M.; Groth, T. Comparative Study of Osteogenic Activity of Multilayers Made of Synthetic and Biogenic Polyelectrolytes. *Macromol. Biosci.* **2017**, *17* (). https://doi.org/ DOI: 10.1002/mabi.201700078.

(16) Alkhoury, H.; Hautmann, A.; Fuhrmann, B.; Syrowatka, F.; Erdmann, F.; Zhou, G.; Stojanović, S.; Najman, S.; Groth, T. Studies on the Mechanisms of Anti-Inflammatory Activity of Heparin-and Hyaluronan-Containing Multilayer Coatings—Targeting NF-KB Signalling Pathway. *Int. J. Mol. Sci.* **2020**, *21*, 3724.

(17) Vikulina, A.; Voronin, D.; Fakhrullin, R.; Vinokurov, V.; Volodkin, D. Naturally Derived Nano- And Micro-Drug Delivery Vehicles: Halloysite, Vaterite and Nanocellulose. *New J. Chem.* **2020**, *44*, 5638−5655.

(18) Volodkin, D. CaCO₃ Templated Micro-Beads and -Capsules for Bioapplications. *Adv. Colloid Interface Sci.* **2014**, *207*, 306−324.

(19) Trushina, D. B.; Bukreeva, T. V.; Antipina, M. N. Size-Controlled Synthesis of Vaterite Calcium Carbonate by the Mixing Method: Aiming for Nanosized Particles. *Cryst. Growth Des.* **2016**, *16*, 1311−1319.

(20) Feoktistova, N. A.; Balabushevich, N. G.; Skirtach, A. G.; Volodkin, D.; Vikulina, A. S. Inter-Protein Interactions Govern Protein Loading into Porous Vaterite CaCO₃ Crystals. *Phys. Chem. Chem. Phys.* **2020**, *22*, 9713−9722.

(21) Svenskaya, Y. I.; Fattah, H.; Inozemtseva, O. A.; Ivanova, A. G.; Shtykov, S. N.; Gorin, D. A.; Parakhonskiy, B. V. Key Parameters for Size- and Shape-Controlled Synthesis of Vaterite Particles. *Cryst. Growth Des.* **2018**, *18*, 331−337.

(22) Vikulina, A. S.; Feoktistova, N. A.; Balabushevich, N. G.; Skirtach, A. G.; Volodkin, D. The Mechanism of Catalase Loading into Porous Vaterite CaCO₃ Crystals by Co-Synthesis. *Phys. Chem. Chem. Phys.* **2018**, *20*, 8822−8831.

(23) Balabushevich, N. G.; Kovalenko, E. A.; Le-Deygen, I. M.; Filatova, L. Y.; Volodkin, D.; Vikulina, A. S. Hybrid CaCO₃-Mucin Crystals: Effective Approach for Loading and Controlled Release of Cationic Drugs. *Mater. Des.* **2019**, *182*, 108020.

(24) Binevski, P. V.; Balabushevich, N. G.; Uvarova, V. I.; Vikulina, A. S.; Volodkin, D. Bio-Friendly Encapsulation of Superoxide Dismutase into Vaterite CaCO₃ Crystals. Enzyme Activity, Release Mechanism, and Perspectives for Ophthalmology. *Colloids Surf., B* **2019**, *181*, 437−449.

(25) Sharma, V.; Vijay, J.; Ganesh, M. R.; Sundaramurthy, A. Multilayer Capsules Encapsulating Nimbin and Doxorubicin for Cancer Chemo-Photothermal Therapy. *Int. J. Pharm.* **2020**, *582*, 119350.

(26) Sergeeva, A.; Vikulina, A. S.; Volodkin, D. Porous Alginate Scaffolds Assembled Using Vaterite CaCO₃ Crystals. *Micromachines* **2019**, *10*, 357.

(27) De Cock, L. J.; Lenoir, J.; De Koker, S.; Vermeersch, V.; Skirtach, A. G.; Dubruel, P.; Adriaens, E.; Vervaet, C.; Remon, J. P.; De Geest, B. G. Mucosal Irritation Potential of Polyelectrolyte Multilayer Capsules. *Biomaterials* **2011**, *32*, 1967−1977.

(28) De Geest, B. G.; Vandenbroucke, R. E.; Guenther, A. M.; Sukhorukov, G. B.; Hennink, W. E.; Sanders, N. N.; Demeester, J.; De Smedt, S. C. Intracellularly Degradable Polyelectrolyte Microcapsules. *Adv. Mater.* **2006**, *18*, 1005−1009.

(29) Strehlow, V.; Lessig, J.; Göse, M.; Reibetanz, U. Development of LbL biopolymer capsules as a delivery system for the multilayer-assembled anti-inflammatory substance α1-antitrypsin. *J. Mater. Chem. B* **2013**, *1*, 3633−3643.

(30) Szarpak, A.; Cui, D.; Dubreuil, F.; De Geest, B. G.; De Cock, L. J.; Picart, C.; Auzeély-Velty, R. Designing Hyaluronic Acid-Based Layer-by-Layer Capsules as a Carrier for Intracellular Drug Delivery. *Biomacromolecules* **2010**, *11*, 713−720.

(31) Sousa, F.; Kreft, O.; Sukhorukov, G. B.; Möhwald, H.; Kokol, V. Biocatalytic Response of Multi-Layer Assembled Collagen/Hyaluronic Acid Nanoengineered Capsules. *J. Microencapsulation* **2014**, *31*, 270−276.

(32) Radhakrishnan, K.; Tripathy, J.; Raichur, A. M. Dual Enzyme Responsive Microcapsules Simulating an "OR" Logic Gate for Biologically Triggered Drug Delivery Applications. *Chem. Commun.* **2013**, *49*, 5390−5392.

(33) Jin, Y.; Liu, W.; Wang, J.; Fang, J.; Gao, H. (Protamine/Dextran Sulfate)6 Microcapules Templated on Biocompatible Calcium Carbonate Microspheres. *Colloids Surf., A* **2009**, *342*, 40−45.

(34) Gnanadhas, D. P.; Ben Thomas, M.; Elango, M.; Raichur, A. M.; Chakravortty, D. Chitosan-Dextran Sulphate Nanocapsule Drug Delivery System as an Effective Therapeutic against Intraphagosomal Pathogen Salmonella. *J. Antimicrob. Chemother.* **2013**, *68*, 2576−2586.

(35) Radhakrishnan, K.; Thomas, M. B.; Pulakkat, S.; Gnanadhas, D. P.; Chakravortty, D.; Raichur, A. M. Stimuli-Responsive Protamine-

Based Biodegradable Nanocapsules for Enhanced Bioavailability and Intracellular Delivery of Anticancer Agents. *J. Nanopart. Res.* **2015**, *17*, 341.

(36) Caruso, F.; Caruso, R. A.; Möhwald, H. Nanoengineering of Inorganic and Hybrid Hollow Spheres by Colloidal Templating. *Science* **1998**, *282*, 1111−1114.

(37) Caruso, F. Hollow Capsule Processing through Colloidal Templating and Self-Assembly. *Chem.—Eur. J.* **2000**, *6*, 413−419.

(38) Volodkin, D. CaCO₃ Templated Micro-Beads and -Capsules for Bioapplications. *Adv. Colloid Interface Sci.* **2014**, *207*, 306−324.

(39) De Geest, B. G.; Déjugnat, C.; Prevot, M.; Sukhorukov, G. B.; Demeester, J.; De Smedt, S. C. Self-Rupturing and Hollow Microcapsules Prepared from Bio-Polyelectrolyte- Coated Microgels. *Adv. Funct. Mater.* **2007**, *17*, 531−537.

(40) Shutava, T. G.; Pattekari, P. P.; Arapov, K. A.; Torchilin, V. P.; Lvov, Y. M. Architectural Layer-by-Layer Assembly of Drug Nanocapsules with PEGylated Polyelectrolytes. *Soft Matter* **2012**, *8*, 9418−9427.

(41) Amancha, K. P.; Balkundi, S.; Lvov, Y.; Hussain, A. Pulmonary Sustained Release of Insulin from Microparticles Composed of Polyelectrolyte Layer-by-Layer Assembly. *Int. J. Pharm.* **2014**, *466*, 96−108.

(42) Santos, A. C.; Pattekari, P.; Jesus, S.; Veiga, F.; Lvov, Y.; Ribeiro, A. J. Sonication-Assisted Layer-by-Layer Assembly for Low Solubility Drug Nanoformulation. *ACS Appl. Mater. Interfaces* **2015**, *7*, 11972−11983.

(43) Shutava, T. G.; Fakhrullin, R. F.; Lvov, Y. M. Spherical and Tubule Nanocarriers for Sustained Drug Release. *Curr. Opin. Pharmacol.* **2014**, *18*, 141−148.

(44) Jeannot, L.; Bell, M.; Ashwell, R.; Volodkin, D.; Vikulina, A. Internal Structure of Matrix-Type Multilayer Capsules Templated on Porous Vaterite CaCO₃ Crystals as Probed by Staining with a Fluorescence Dye. *Micromachines* **2018**, *9*, 547.

(45) Sarode, A.; Annapragada, A.; Guo, J.; Mitragotri, S. Layered Self-Assemblies for Controlled Drug Delivery: A Translational Overview. *Biomaterials* **2020**, *242*, 119929.

(46) Feoktistova, N.; Rose, J.; Prokopović, V. Z.; Vikulina, A. S.; Skirtach, A.; Volodkin, D. Controlling the Vaterite CaCO₃ Crystal Pores. Design of Tailor-Made Polymer Based Microcapsules by Hard Templating. *Langmuir* **2016**, *32*, 4229−4238.

(47) Feoktistova, N. A.; Vikulina, A. S.; Balabushevich, N. G.; Skirtach, A. G.; Volodkin, D. Bioactivity of Catalase Loaded into Vaterite CaCO₃ Crystals via Adsorption and Co-Synthesis. *Mater. Des.* **2020**, *185*, 108223.

(48) Balabushevich, N. G.; Kovalenko, E. A.; Mikhalchik, E. V.; Filatova, L. Y.; Volodkin, D.; Vikulina, A. S. Mucin Adsorption on Vaterite CaCO₃ Microcrystals for the Prediction of Mucoadhesive Properties. *J. Colloid Interface Sci.* **2019**, *545*, 330−339.

(49) Bromfield, S. M.; Wilde, E.; Smith, D. K. Heparin Sensing and Binding-Taking Supramolecular Chemistry towards Clinical Applications. *Chem. Soc. Rev.* **2013**, *42*, 9184−9195.

(50) Zhao, Q.; Li, B. PH-Controlled Drug Loading and Release from Biodegradable Microcapsules. *Nanotechnology, Biology and Medicine* **2008**, *4*, 302−310.

(51) Shchukin, D. G.; Patel, A. A.; Sukhorukov, G. B.; Lvov, Y. M. Nanoassembly of Biodegradable Microcapsules for DNA Encasing. *J. Am. Chem. Soc.* **2004**, *126*, 3374−3375.

(52) Somosi, Z.; Pavlovic, M.; Pálinkó, I.; Szilágyi, I. Effect of Polyelectrolyte Mono- and Bilayer Formation on the Colloidal Stability of Layered Double Hydroxide Nanoparticles. *Nanomaterials* **2018**, *8*, 986.

(53) Köhler, K.; Biesheuvel, P. M.; Weinkamer, R.; Möhwald, H.; Sukhorukov, G. B. Salt-Induced Swelling-to-Shrinking Transition in Polyelectrolyte Multilayer Capsules. *Phys. Rev. Lett.* **2006**, *97*, 188301.

(54) She, S.; Shan, B.; Li, Q.; Tong, W.; Gao, C. Phenomenon and Mechanism of Capsule Shrinking in Alkaline Solution Containing Calcium Ions. *J. Phys. Chem. B* **2012**, *116*, 13561−13567.

(55) Tong, W.; She, S.; Xie, L.; Gao, C. High Efficient Loading and Controlled Release of Low-Molecular-Weight Drugs by Combination of Spontaneous Deposition and Heat-Induced Shrinkage of Multilayer Capsules. *Soft Matter* **2011**, *7*, 8258−8265.

(56) Leporatti, S.; Gao, C.; Voigt, A.; Donath, E.; Möhwald, H. Shrinking of Ultrathin Polyelectrolyte Multilayer Capsules upon Annealing: A Confocal Laser Scanning Microscopy and Scanning Force Microscopy Study. *Eur. Phys. J. E: Soft Matter Biol. Phys.* **2001**, *5*, 13−20.

(57) Trushina, D. B.; Bukreeva, T. V.; Borodina, T. N.; Belova, D. D.; Belyakov, S.; Antipina, M. N. Heat-Driven Size Reduction of Biodegradable Polyelectrolyte Multilayer Hollow Capsules Assembled on CaCO₃ Template. *Colloids Surf., B* **2018**, *170*, 312−321.

(58) Caruso, F.; Schüler, C. Enzyme Multilayers on Colloid Particles: Assembly, Stability, and Enzymatic Activity. *Langmuir* **2000**, *16*, 9595−9603.

(59) Ambrosi, M.; Fratini, E.; Baglioni, P.; Vannucci, C.; Bartolini, A.; Pintens, A.; Smets, J. Microcapsules for Confining Fluids: Prediction of Shell Stability from Advanced SAXS Investigations. *J. Phys. Chem. C* **2016**, *120*, 13514−13522.

(60) Volodkin, D.; Mohwald, H.; Voegel, J.-C.; Ball, V. Coating of Negatively Charged Liposomes by Polylysine: Drug Release Study. *J. Controlled Release* **2007**, *117*, 111−120.